ON-ORBIT THERMAL PERFORMANCE OF A SUBMILLIMETER TELESCOPE PRIMARY REFLECTOR PANEL

G. Tsuyuki*and L. French*”
Jet Propulsion Laboratory
California Institute of Technology
Pasadena, California

Abstract

A detailed thermal analysis has been performed for a panel of a segmented primary mirror which is closest to the high side of the telescope sunshade, This panel was selected because the spatial temperature distribution was expected to be the worst. The JPL90- 10 primary reflector panel configuration was investigated because of its superior figure error performance in ground-based testing. The analysis utilizes a two TMM approach: i) a detailed sub-TMM of a selected panel is generated with ‘specifically designed software; ii) this detailed sub-model is then incorporated into the system-level model (removing the gross nodalization for the selected panel). Since steady-state simulations are performed, the resulting TMM is not extremely costly to implement.

Nomenclature

BCS	Block coordinate system
ESA	European Space Agency
FLUINT	Fluid integrator
GMM	Geometric math model
Gr/Ep	Graphite/epoxy
Gr/Ph	Graphite/phenolic
IR	Infrared
ISRS	Inflatable space rigidized structure
JPL	Jet Propulsion Laboratory
MLI	Multi-layer insulation
NEVADA	Net Verification and Determination Analyzer
RADK	Radiation conductor
SINDA85	Systems Improved Numerical Difference Analyzer 1985
SMILS	Submillimeter Imager and Line Survey
TMM	Thermal math model
TRASYS	Thermal Radiation Analysis System

Greek

α_s	Solar absorptivity
ϵ	Hemispherical emissivity

Introduction

An optimized thermal design for the SMILS telescope system has been developed.’ This design has demonstrated that the expected on-orbit lateral temperature gradient in the primary reflector has been minimized. Depending upon the primary reflector construction, the lateral gradient (measured between the primary reflector panels nearest the high and low sides of the telescope sunshade) ranges between 2.2 and 2.4K. The on-orbit primary reflector temperature is expected to range between 91 K and 99K. These estimates are based upon steady-state results from a system-level TMM of the SMILS telescope, and this model represents each primary reflector panel with two nodes

•Technical Group Leader, Member AIAA

** Member of Technical Staff

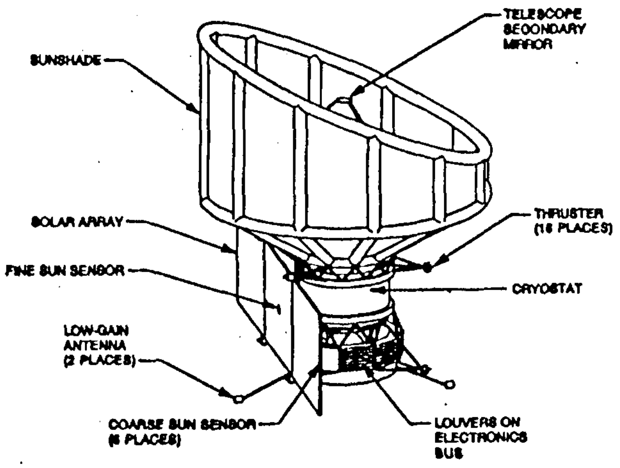

Figure 1 - SMILS telescope configuration

(mirror and back side). However, there is not sufficient nodal granularity to deduce a spatial temperature distribution for an individual panel. Hence, the lateral thermal gradient that is predicted by the system-level TMM may be underestimated since, a one node representation of the mirror side will tend to average the spatial temperature variation on the panel. The actual spatial temperature distribution on each panel is critical in understanding the thermal distortion and hence the optical performance, Since SMILS observations are performed for wavelengths between 100 to 800 μm, the figure error of the primary mirror must be at least an order of magnitude less than observation wavelengths, The current requirement is $4.5 \mu m$. Spatial temperature gradients within a primary reflector panel must be minimized in order for this figure error requirement to be attained. In addition, understanding a panel's spatial temperature distribution and its driving parameters are crucial in minimizing figure error due to thermal distortions.

Approach

SMILS Telescope Thermal Design

The most visible feature of the thermal design is the inflatable sunshade (see Fig. 1). This sunshade is stowed in a container above the telescope cryostat during launch/ascent. Once in orbit, the ISRS members are inflated and cured by solar heating. MLI blankets are then drawn between the ISRS members to complete the sunshade deployment. The conical portion implements 15 layer MLI blankets whereas the cylindrical portion uses 6 layer MLI blankets. The sunshade has an appearance of a scarfed cylinder in order to meet Sun and Earth avoidance requirements. The telescope is able to pitch toward or away from the Sun by 25°, but incident Sun is not allowed on the interior of the sunshade or primary reflector. In addition, the primary reflector may never view the Earth, although Earth albedo and IR fluxes may be incident upon the interior of the sunshade. Thermal control coatings play a major role in thermally isolating the primary reflector from its environment. The portion of the sunshade exterior that is illuminated by the Sun has an exterior layer of aluminized Teflon (with the Teflon side facing outward) which minimizes the absorbed direct solar flux. The. sunshade exterior which is not illuminated has an exterior layer of aluminized Kapton (aluminized side facing outward). These exterior thermal control surfaces serve to isolate the telescope from the thermal environment. The sunshade interior utilizes the same aluminized Kapton as the non-illuminated sunshade exterior. This reduces the thermal coupling between the sunshade interior and primary reflector. The back support structure of the primary structure is wrapped with 20 layer MLI blankets and the exterior layer is the same aluminized Kapton used on the non-illuminated sunshade exterior.

System-Level Telescope TMM

The system-level TMM encompasses the sunshade, primary reflector, secondary reflector (with support truss), back support structure,

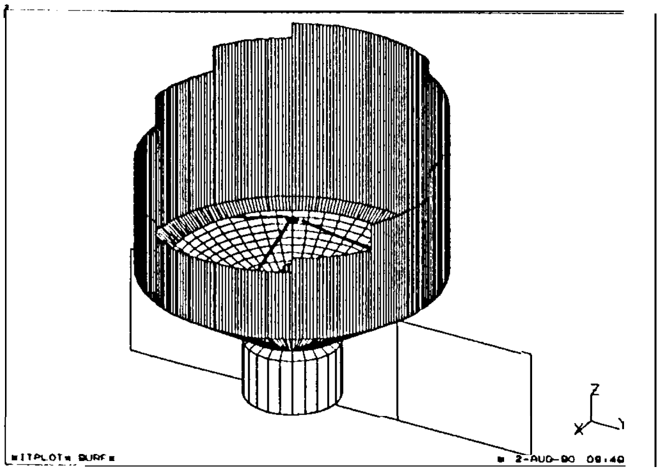

Figure 2- System-level telescope TMM

optical bench MLI, and sunshade spool MLI. The model is composed on 178 nodes (See Fig 2). Each primary reflector panel is represented by two nodes (mirror and back side). The sunshade is divided circumferentially into twelve equal divisions and axially where the sunshade transitions from cylindrical to conical, The back support structure is not explicit] y modeled, but its thermal capacitance is added to the inner layer of the back support structure MLI. The normal heat transfer for a 6 and 15 layer blanket is modeled by extrapolating effective thermal conductivity data for 10 layer and 20 layer blankets, respective y.[2,3] Lateral MLI blanket heat transfer is modeled within the sunshade. The blankets between any pair of ISRS members are thermally connected to these members, The member temperatures are driven as boundary nodes based on thermal analyses conducted by ESA.[4] All other conductive heat paths (i.e. back support conduction, secondary reflector support conduction, primary reflector attach point to back support structure, etc.) have been neglected. Radiative edge effects between primary reflector panels have been ignored. The baseline mission trajectory is a highly elliptical 1,000 km x 70,000 km orbit. Through the optimization process, the pitch angle of the. telescope has been identified as the most dominant thermal parameter.[1] In recognition of this finding, two steady-state cases were used in characterizing the thermal design during optimization: i) telescope pitched 25° toward the Sun (no Earth albedo or IR heating); and ii) telescope pitched 25° away from the Sun (no Earth albedo or IR heating). These attitudes are depicted in Figs. 3 and 4. Previous analysis has demonstrated that the omission of the Earth albedo and IR heating results in a decrease of - 6K in temporal temperature for the primary reflector.[1] Hence omission of the Earth albedo and IR heating does not significantly reduce the rigor of the analysis, but it greatly simplifies the analysis.

Detailed Primary Reflector Panel Sub-TMM

Current panel fabrication produces spherically-shaped hexagonal panels. Typically, the panel is a sandwich construction of Gr/Ep face sheets and a core material. The core material may be

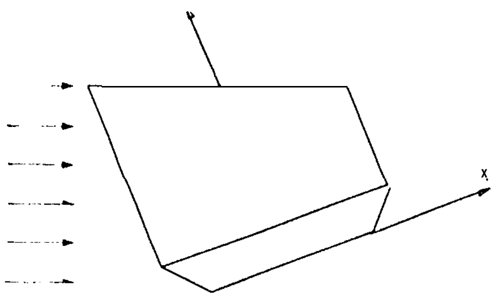

Figure 3 - Cold case: Telescope pitched **250** toward Sun

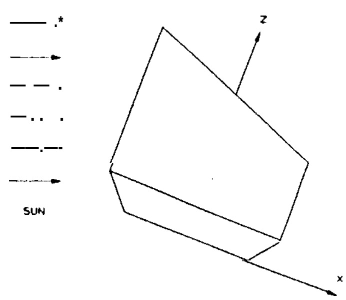

Figure 4 - Hot Case: Telescope pitched **25°** away from Sun

Table 1- Panel Sub-Model Generator Thermophysical Property Database

Material	Thermal Conductivity	Specific Heat
Hexcel 1	in-plane, normal	yes
UHM/RS-3	in-plane, normal	to be added
Al Flex Core CRIII	in-plane, normal	yes
Al Dbl Flex Core 5052	in-plane	yes
T300/Phenolic	in-plane, normal	yes
E-Glass/Phenolic	in-plane	to be added

metallic (aluminum) or non-metallic (composite material) in nature. A wide variety of panel configurations are available, but the most promising configuration is JPL90- 10.[5] It is composed of UH 155/F 155 Gr/Ep facesheets and T300 Gr/Ph core.

Generic Hexagonal Panel Sub-TMM Generator

Since there is a wide breadth of available panel configurations, a TMM generator was developed to be able to meet the thermal analysis needs in a timely fashion. The TMM generator is a FORTRAN program that maybe executed on a micro-computer or VAX mainframe.[6] The generator is interactive and queries the user for number of TMM nodes, panel edge dimension, and facesheet and core thicknesses. The TMM analyzer input format is compatible with SINDA85/FLUINT, Version 2.2 .[7] Currently, the generator creates TMMs for flat panels although it may be altered to include curvature. The nodalization methodology is currently based upon the structural analysis approach, and the general node shape is hexagonal (edge nodes are portions of hexagons). Nodalization of each layer (i.e. facesheet or core material) through the panel thickness is consistent with adjacent layers, but the number of nodes per layer may be varied (but in the same manner for all layers). There is a thermophysical properties database (Table 1) for many of the panel materials, and these. properties are temperature dependent based on various sources.[3,8] The generated TMM models in-plane and normal-to-plane conduction with different thermal conductivities. By using SINDA85/FLUINT, the panel "sub-model" may easily incorporated into the system-level model,

Generic Hexagonal Panel Sub-GMM Generator

When a particular panel is finely nodalized, the radiation interchange between the detailed panel and the surrounding surfaces must be determined. In addition, it may be necessary to determine the absorbed environmental heating. These RADKs and absorbed heating rates are used as input to the panel TMM. Once again, a geometric generator was developed in concert with the TMM generator to be able to perform a timely thermal analysis for any particular panel configuration. The GMM generator is also a FORTRAN program that may be used on the micro-computer or the VAX mainframe. The GMM analyzer format is compatible with TRASYS Version 22P.[9] The GMM is largely composed of triangular elements since TRASYS cannot model hexagonal surfaces discretely. However, the corresponding triangular elements are combined within TRASYS to provide

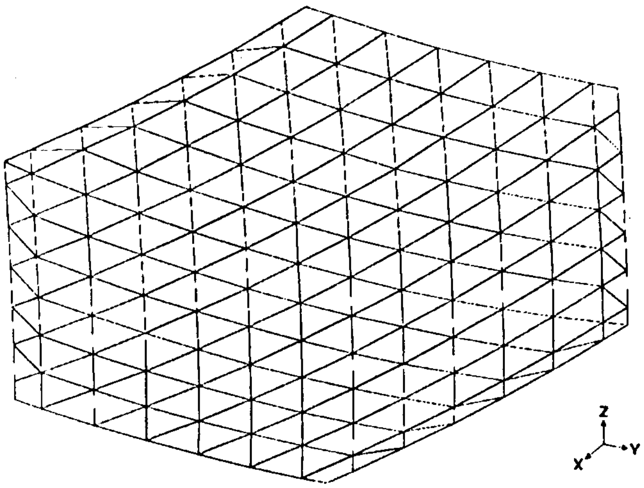

Figure 5- Panel sub-TMM nodalization

radiation interchanged factors and absorbed heating for the hexagonal TMM nodes as shown in Fig. 5. The core layer is not modeled in the GMM since it is not an exterior surface. The panel shape may be spherical or parabolic. For spherical panels, the generator will ask the user to input the radius of curvature. Parabolic panels are constructed assuming the center of the panel is the vertex, and the user is asked to input the F/D ratio. An off-axis parabolic panel option can be easily incorporated into the generator, but this capability does not currently exist. Other parameters that the user will be asked to input include: panel point-to-point or flat-to-flat dimension, number of nodal divisions along a panel edge, and mirror and back side optical properties, A local coordinate system is selected. Surfaces along the ±y-axis are placed into a separate BCS, and the other surfaces lying in the +x/ + y quadrant are placed into another BCS. The entire panel is constructed by surface imaging the +x/ + y quadrant surfaces into the -x/+ y, -x/-y, and +x/-y quadrants (see Fig. 6). This modeling methodology must be kept in mind when this GMM is incorporated into a system-level model.

Detailed Panel Thermal Sub-Model Incorporated into System-Level Thermal Model

The primary reflector panel nearest the high side of the sunshade was selected for this analysis. Since this panel is expected to have the most variation in view to space as one moves from the panel edge closest to the sunshade toward the center of the primary reflector. A panel sub-GMM and TMM were constructed based on the attributes which are shown in Table 2. First, the panel sub-GMM is incorporated into the system-level GMM (See Fig. 7). Since TRASYS did not at that time accommodate sub-models readily, the chore of integrating the panel sub-model to take advantage of its symmetry is cumbersome. However, there are great benefits in reduced execution time by using symmetry. TRASYS is used to calculate RADKs between the detailed panel nodalization and the surrounding nodes from the system-level model, For this analysis, orbital heating was not performed since Earth albedo and planetary heating was ignored, Therefore, the absorbed direct solar heating developed for the system-level GMM was still applicable. However, if a transient orbital analysis is undertaken, orbital heating with the panel sub-GMM integrated into the system-level GMM must be performed.

The sub-TMM developed from the TMM generator is much more easier to incorporate into the system-level TMM since SINDA85/FLUINT can manage sub-models. The RADKs calculated from TRASYS are retrieved into SINDA85/FLUINT through use of the 'INCLUDE' macro.

Analysis

Cases Investigated

The steady-state hot and cold cases were investigated. In either case, the Earth albedo

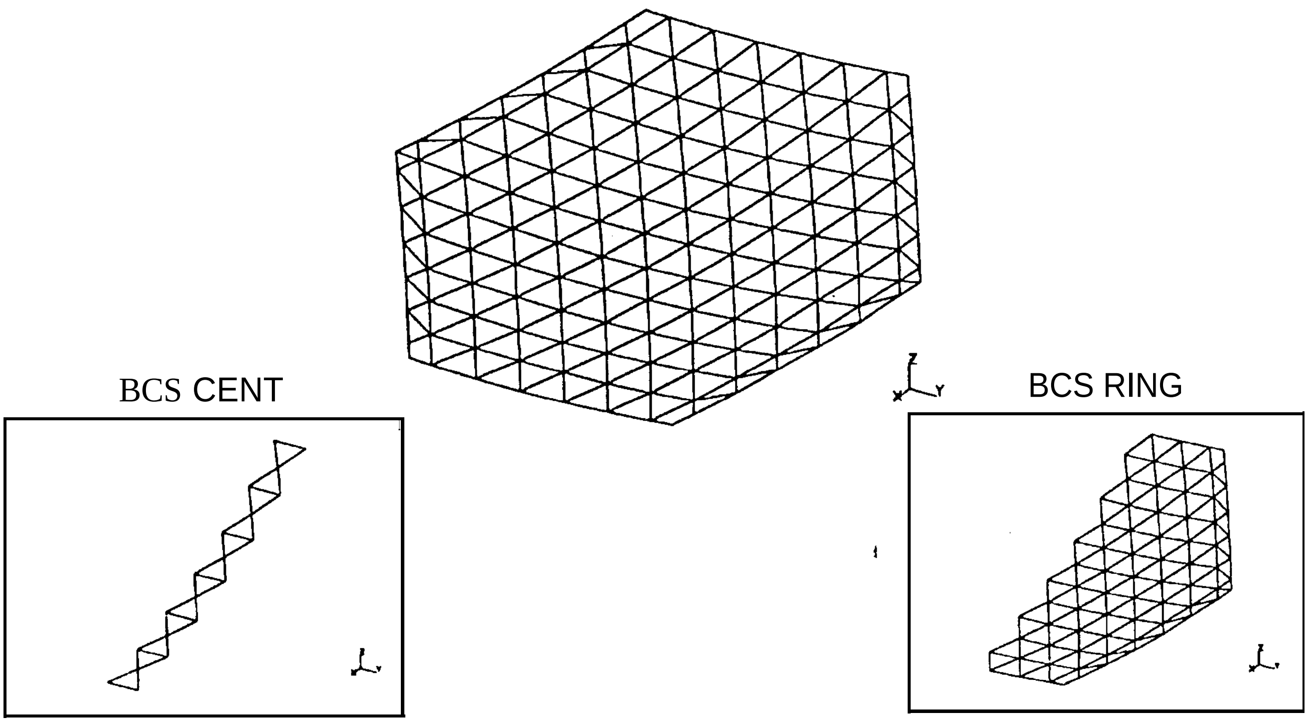

Figure6 -Construction methodology **for panel sub-GMM**

and IR heating were neglected. The system-level analysis has demonstrated that the thermal effect of the Earth is rather small compared to the pitching of the telescope. The cold case presents the minimum sunshade projected area to the Sun, whereas, in the hot case, the projected sunshade area toward the Sun is a maximum.

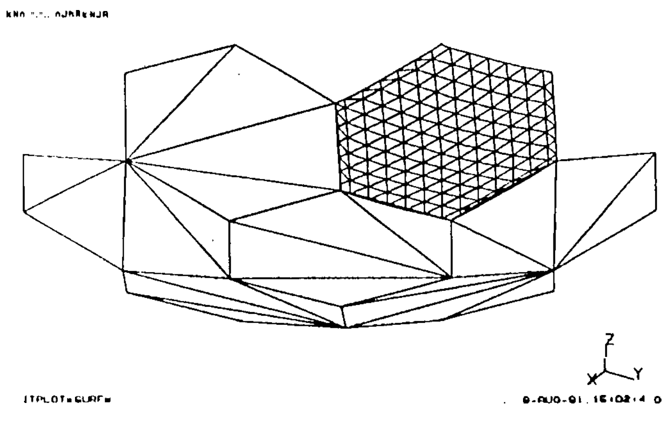

Figure 7 - Panel sub-model integrated into system-level model (primary reflector only shown)

Results

Cold Case

The detailed panel was extremely isothermal. Its steady-state mirror spatial temperature varied between 99. 88K and 99.91K. Temperatures were so uniform that an isotherm plot of the panel would be of no particular use. The temperature gradient through the panel thickness was less than 0.02K. The primary reflector lateral temperature gradient was 3.5K, with spatial temperatures varying from 96.4K to 99.9K.

Hot Case

As with the cold case, the detailed panel was very isothermal, and again, no isotherm plot is given. The mirror spatial temperature varied

Table 2- Panel Sub-Model Attributes

Attribute	Value
Flat-to-Flat Dimension	1.256 m
Radius of Curvature	2.92 m
Face Sheet Thickness	0.00174 m
Core Thickness	0.0254 m
Nodes Along Panel Edge	7
Total Nodes	381
Mirror Side α_s/ϵ	0.14/0.03
Back Side α_s/ϵ	o. 14/0.03

between 105.21K and 105. 19K. As with the cold case, the gradient through the thickness was larger than the cold case value, but it is still small (< 0.07K). The lateral temperature gradient of the primary reflector was 3.3K, and the primary reflector temperature ranged between 101. 9K and 105.2K.

Discussion of Results

The most obvious result is the isothermality of the panel. Since the mirror side of the panel, and the sunshade are both highly reflective, each panel node absorbs very little heat. Not only is the absorbed heat minimal, but it is very uniform. The TMM network was examined to determine the amount of heat flowing into each panel node. Since the panel node areas are not uniform, the heat flux (heat flow per unit area) was compiled for the panel vertex and center nodes. The fluxes are depicted in Fig. 8. For the cold case, the selected panel node heat fluxes vary from 0.319 W/m^2 to 0.347 W/m^2, and for the cold case, these fluxes varied

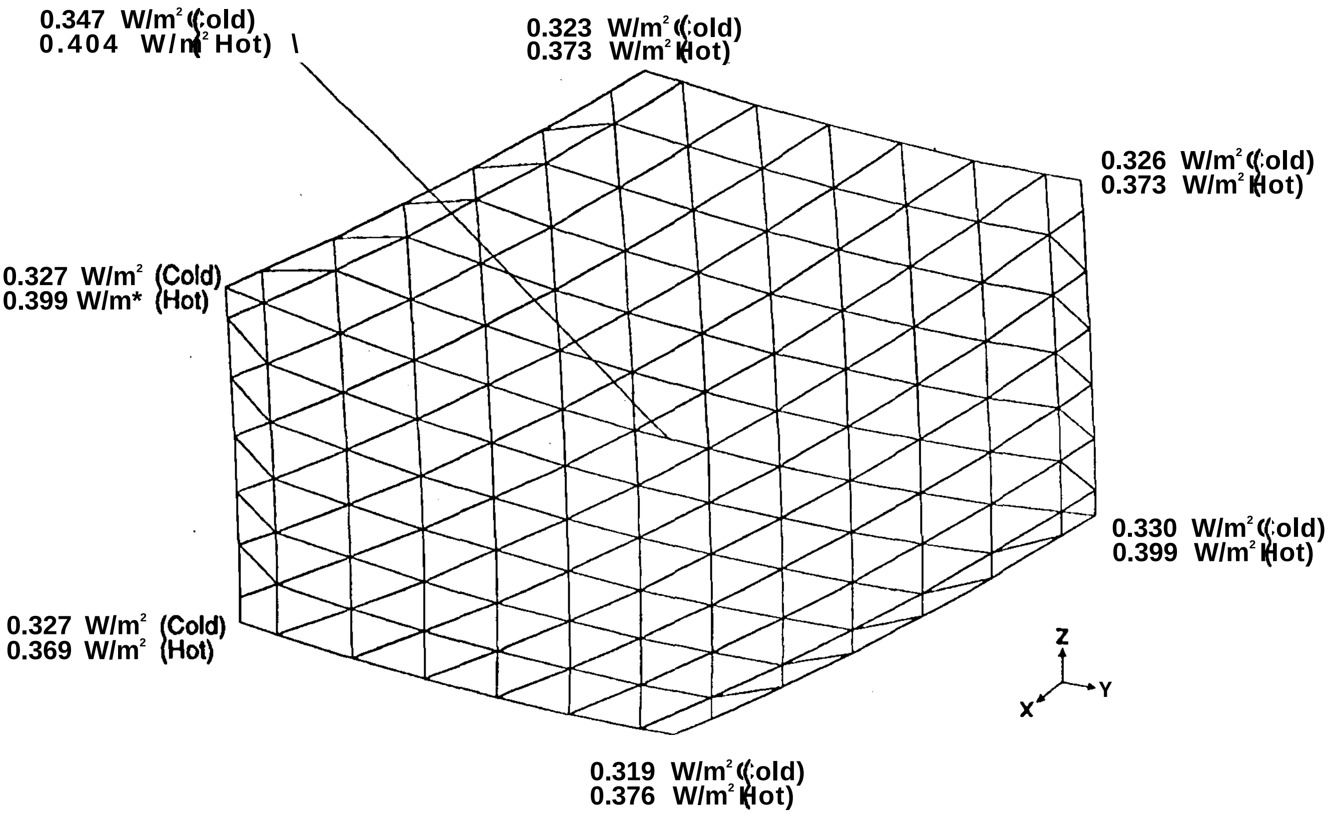

Figure 8 -Total heat flux into vertex and center panel nodes

Table 3- Comparison between system-level and detailed panel TMMs

Primary Reflector Attribute	System-level TMM	Detailed panel TMM
Temperature	90.8K to 93.2K (cold) 96.4K to 98.6K (hot)	96.4K to 99.9K (cold) 101.9K to 105.2K (hot)
Through-the Thickness Gradient	0.03K (cold) O. 14K (hot)	0.02K (cold) 0.07K (hot)

between 0.369 W/m* and 0.404 W/m^2. In absolute terms, the heat flow into these particular panel nodes ranged between 0.5 mW to 2.0 mW for the cold case, and 0.7 mW to 2.6 mW for the hot case. Although, the heat flux for the center node was slightly larger than the vertex nodes, the RADK to space was also slightly larger. Hence, the resulting panel temperatures are the same.

A comparison between the system-level and detailed panel TMMs indicate that the system-level model tends to provide temperatures that are colder than the detailed panel model. This comparison is shown in Table 3. As expected, the system-level model underestimates the primary reflector lateral gradient. However, the through-the-thickness gradient for the hot case is overestimated by the system-level model. The difference in this gradient prediction is within the uncertainty of modeling, and it is not deemed to be a serious problem.

The spatial panel temperature variations are virtually absent, and this implies that the resulting figure error from thermal distortions will be small. However, this anal ysis has been predicated on one crucial assumption: The radiative behavior of the highly reflective surfaces are diffuse. In actuality, the highly reflective surfaces are more likely to be specular. It is possible that the specular nature of the mirror side of the primary reflector can destroy the spatial temperature uniformity which is currently seen. Future panel analyses should utilize the NEVADA radiation analyzer since it has specular modeling capability.'0

Acknowledgements

The work described in this paper was conducted by the Jet Propulsion Laboratory, California Institute of Technology under a contract with the National Aeronautics and Space Administration. The authors would like to express their appreciation to Richard Helms and Chris Porter for their useful technical comments and discussions throughout the duration of this work.

References

1. Tsuyuki, G. and Cohen, E. "Thermal Design Optimization of a Segmented GFRP Primary Reflector for a Submillimeter Telescope, " *Design of Optical Instruments*, David M. Aikens, Victor L. Genberg, Gary C. Krumweide, Michael J. Thomas, Editors, Proc. SPIE 1690, Pp. 265-272, 1992.

2. Orbiter Midsection/Payload Bay Thermal Math Model Description (Model No. SSX001D), Johnson Space Center, Houston, Texas, June 1983.

3. *Spacecraft Thermal Control Design Data*, ESA (TST-02), European Space Agency,

Noordwijk, Netherlands, 1984.

4, *FIRST Inflatable **Thermal Sheild,** Phase 1-Final Report,* ESA Contract Report 6324/85/NL/PB(SC), June 1987.

5. Porter, C. C., "LDR/PSR Materials List", personal communication, Jet Propulsion Laboratory, Pasadena, California, August 1991.

6. French, L., "User's Memo for Hexagonal Panel Thermal Math Model Generator, " personal communication, Jet Propulsion Laboratory, Pasadena, California, August 6, 1991.

7. *SINDA '85/FL UINT, Systems Improved Numerical Differencing Analyzer and Fluid Integrator, Version 2.2,* COSMIC program MSC-21528, University of Georgia, Athens, Georgia, November "1987.

8. Thermal Properties of Gr/E PBD Materials, Rockwell International Internal Document 75-993-1357, Downey, California, February 5, 1975

9. Thermal Radiation Analyzer System (TRASYS) User's Manual, Johnson Space Center, Houston, Texas, December 1987.

10. *Net Verification and Determination Analyzer (NEVADA) User's Manual,* Turner Associates Consultants, Incline Village, Nevada, April 1990.